



SUPPLEMENTARY MATERIAL TO  
**Copper-based nanoparticles prepared from copper(II) acetate  
bipyridine complex**

TATIANA A. LASTOVINA<sup>1\*</sup>, ANDRIY P. BUDNYK<sup>1</sup>, GEVORG A. KHAISHBASHEV<sup>1</sup>,  
EGOR A. KUDRYAVTSEV<sup>2</sup> and ALEXANDER V. SOLDATOV<sup>1</sup>

<sup>1</sup>International Research Center "Smart materials", Southern Federal University, 344090, 5,  
Zorge Str., Rostov-on-Don, Russia and <sup>2</sup>Joint Research Center „Diagnostics of structure and  
properties of nanomaterials“, Belgorod National Research University, 308015, 85, Pobedy  
Str., Belgorod, Russia

*J. Serb. Chem. Soc.* 81 (7) (2016) 751–762

A SELECTION OF COPPER PRECURSORS

TABLE S-I. Examples of Cu(II) precursors used for the synthesis of Cu, CuO or Cu<sub>2</sub>O NPs

Compound	Reagents / Method	Particles	Ref.
CuCl <sub>2</sub>	Chemical reduction by NaBH <sub>4</sub> in methanol in Ar atmosphere	Cu NPs, 5–15 nm, spherical	1
CuCl <sub>2</sub> ·2H <sub>2</sub> O	Chemical reduction by L-ascorbic acid at 80 °C until change in color	Cu NPs, 2 nm, spherical	2
Cu-(N <sub>2</sub> H <sub>3</sub> COO) <sub>2</sub> ·2H <sub>2</sub> O from CuCl <sub>2</sub>	Thermal Process: 80 °C for 3 h in Ar atmosphere. Sonochemical Process: 100 W cm <sup>-2</sup> ultrasound radiation for 3 h in water	Cu NPs, 200–300 nm, irregular Cu NPs, 50 nm, porous & irregular	3
CuSO <sub>4</sub>	Chemical reduction by NaBH <sub>4</sub> in water and stabilization by C <sub>6</sub> H <sub>5</sub> O <sub>7</sub> Na <sub>3</sub>	Cu NPs, 70 nm, irregular	4
Cu(NO <sub>3</sub> ) <sub>2</sub>	Chemical reduction by NaBH <sub>4</sub> in methanol and stabilization by PEG	Cu NPs, 2 nm, round-like	5
Cu(NO <sub>3</sub> ) <sub>2</sub> ·H <sub>2</sub> O	Precipitation–pyrolysis by (1) sol–gel in ethanol/propanol, (2) calcination at 200–500 °C for 1 h	CuO NPs, 30 nm (XRD)	6
CuSO <sub>4</sub> ·5H <sub>2</sub> O	Precipitation–pyrolysis by (1) addition of NaOH in C <sub>6</sub> H <sub>5</sub> O <sub>7</sub> Na <sub>3</sub> , (2) calcination at 500 °C for 3 h	CuO NPs, 19 nm (XRD), 20–50 nm (TEM) irregular	7
A. CuCO <sub>3</sub> ·Cu(OH) <sub>2</sub> from Cu(OAc) <sub>2</sub> B. Cu(OH) <sub>2</sub> & CuSO <sub>4</sub>	Precipitation–pyrolysis by (1) addition of aqueous (NH <sub>4</sub> ) <sub>2</sub> CO <sub>3</sub> , (2) calcination at 200–500 °C for 3 h	CuO NPs 8–26 nm (XRD), CuO nanorods 30x100 nm	8

\*Corresponding author. E-mail: lastovina@sfedu.ru

TABLE S-I. Continued

Compound	Reagents / Method	Particles	Ref.
CuSO <sub>4</sub> ·5H <sub>2</sub> O	Hydrothermal microwave-assistant in C <sub>6</sub> H <sub>12</sub> O <sub>6</sub> ·H <sub>2</sub> O, C <sub>4</sub> H <sub>4</sub> O <sub>6</sub> KNa·4H <sub>2</sub> O & PEG mixture at pH=12 (NaOH), 700 W stove at 95 °C for 1 h.	Cu <sub>2</sub> O NPs 400–680 nm, different shapes	9
CuSO <sub>4</sub> ·5H <sub>2</sub> O	Solution-phase in PVP, NaH <sub>2</sub> C <sub>6</sub> H <sub>5</sub> O <sub>7</sub> , Na <sub>2</sub> CO <sub>3</sub> & glucose mixture at 80 °C for 2 h	Cu <sub>2</sub> O NPs 300–500 nm, different shapes	10

## FORMATION OF COPPER(II) ACETATE BIPYRIDINE COMPLEX

The Cu(II) acetate bipyridine complex was synthesized from parent Cu(II) acetate (Alfa Aesar) according to a method proposed by Koo.<sup>11</sup> The FTIR spectra of the parent compound and the formed complex are presented in Fig. S-1. The spectra were measured in transmittance mode on an FSM-1202 FTIR spectrometer (InfraSpec) in air. The sample powder was mixed with KBr powder in a weight ratio of 1:200 and pressed into a disc of 1 mm thickness. The spectrum of a reference KBr disc was subtracted from the spectra.

The main spectroscopic features originate from vibrations of the acetate group with participation from adsorbed water. The spectrum of Cu(II) acetate bipyridine contained characteristic bands, mentioned by Koo in his work:<sup>11</sup> 2923, 1580, 1400, 1375, 1317, 1248, 1027, 923, 771 and 676 cm<sup>-1</sup>. They are highlighted in Fig. S-1 by asterisks. In the region of 600–500 cm<sup>-1</sup>, there were some bands related to Cu–O bond stretching vibrations (clearly visible for Cu(II) acetate and less pronounced for Cu(II) acetate bipyridine).

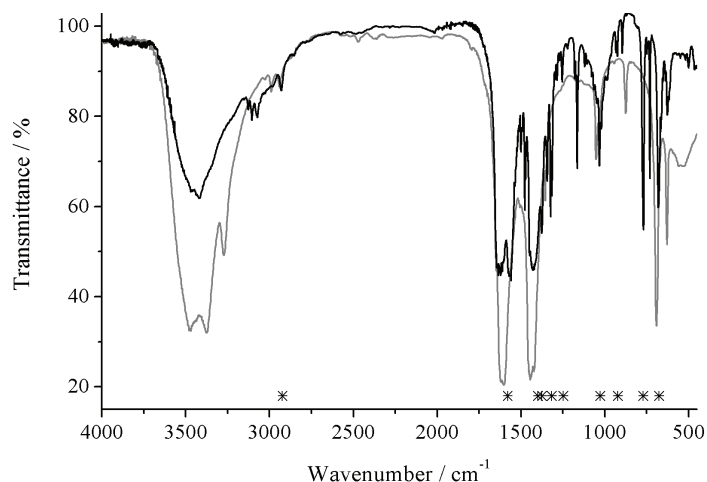


Fig. S-1. FTIR spectra of Cu(II) acetate bipyridine (black) and Cu(II) acetate (grey). The asterisks mark the positions of additional vibrations for Cu(II) acetate bipyridine.<sup>11</sup>

Optical spectra of the precursors were collected in the diffuse reflectance mode on a Shimadzu UV2600 spectrophotometer equipped with an integrating sphere. For the measurements, the compounds were mixed with BaSO<sub>4</sub> and filled into a standard UV cuvette. The spectrum of Cu(II) acetate bipyridine (black) obtained in this work, and both precursors Cu(II) acetate (grey) and 2,2'-bipyridine (light grey) presented in % of reflectance values are reported in Fig. S-2. The difference in total intensity of the reflectance relates to different quantities of samples exposed to light.

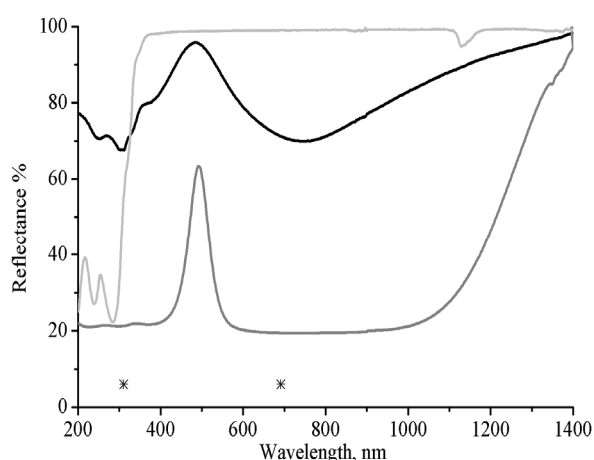


Fig. S-2. DRUV-Vis-NIR spectra of Cu(II) acetate bipyridine (black), Cu(II) acetate (grey) and 2,2'-bipyridine (light grey). The asterisks mark the band positions for Cu(II) acetate bipyridine.<sup>11</sup>

In his work, Koo<sup>11</sup> reported two UV/Vis bands at 310 and 691 nm, which were measured in DMSO-*d*<sub>6</sub> solution. Both bands comply well with the spectral profile of Cu(II) acetate bipyridine in Fig. S-2. In this regard, some comparative comments should be mentioned as well.

Concerning the spectrum of the Cu(II) acetate precursor, the wide band stretching from red to the NIR could undoubtedly be assigned to d-d transitions occurring in Cu, while the high energy band below 400 nm was attributed to acetate-to-copper LCMT transitions comparing to the free ligand bands.<sup>12</sup> As far as the spectrum of 2,2'-bipyridine is concerned, the two clearly distinguished peaks at 237 and 283 nm originated from  $\pi$ -transitions and could be evidence for the prevalence of the *trans*-form in the dry precursor.<sup>13</sup> It was also shown<sup>14</sup> that in metal chelate compounds, the splitting of a higher wavelength  $\pi$ -band (called  $\pi_1$ -band) may occur due to vibrational fine structures.

## CHARACTERIZATION OF THE COPPER AND COPPER OXIDE NANOPARTICLES

The powder XRD patterns for the Cu/Cu<sub>2</sub>O NPs prepared by microwave-assisted polyol synthesis at 185 and 200 °C are presented in Fig. S-3. If the patterns are matched (subtracting baseline), it becomes clear that synthesis at higher temperature results in an almost 2-times decrease in the intensity for reflexes from the Cu NPs, while does not affect appreciably the characteristic reflex (111) from the Cu<sub>2</sub>O NPs. The observed difference could be attributed to the improved crystallinity of the metal particles obtained at the higher temperature.

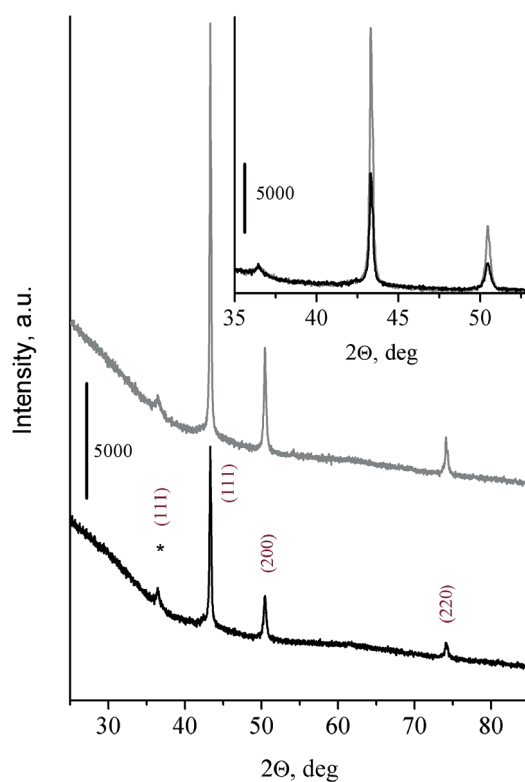


Fig. S-3. XRD pattern of Cu/Cu<sub>2</sub>O NPs prepared by microwave-assisted polyol synthesis at 185 °C (grey) and 200 °C (black). The inset shows the same patterns matched for comparison of the reflex intensities. The asterisk marks the reflex attributed to the Cu<sub>2</sub>O phase.

The TEM images for CuO and Cu/Cu<sub>2</sub>O (185 °C) NPs are presented here in Figs. S-4 and S-5 at a higher magnification than in the main text with the aim to make the details more obvious, while, the same set of analysis are given in Fig. S-6 for the Cu<sub>2</sub>O sample obtained at 200 °C. Figure S-7 shows the formation of particles with a round-like shape having an average size of 95.3 nm. These particles appear to be more agglomerated than those prepared at 185 °C are.

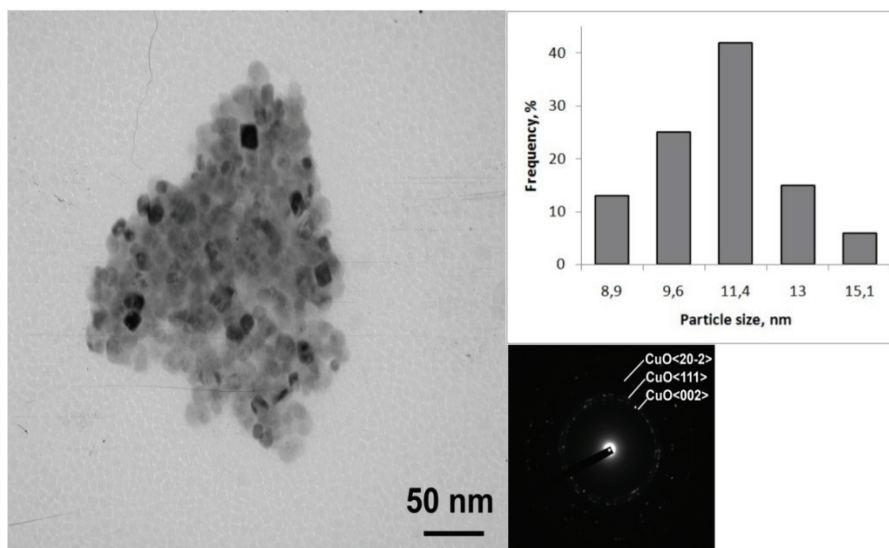


Fig. S-4. TEM image, SAED image and histogram of the size distribution of CuO NPs prepared by the solvothermal method. See text for details.

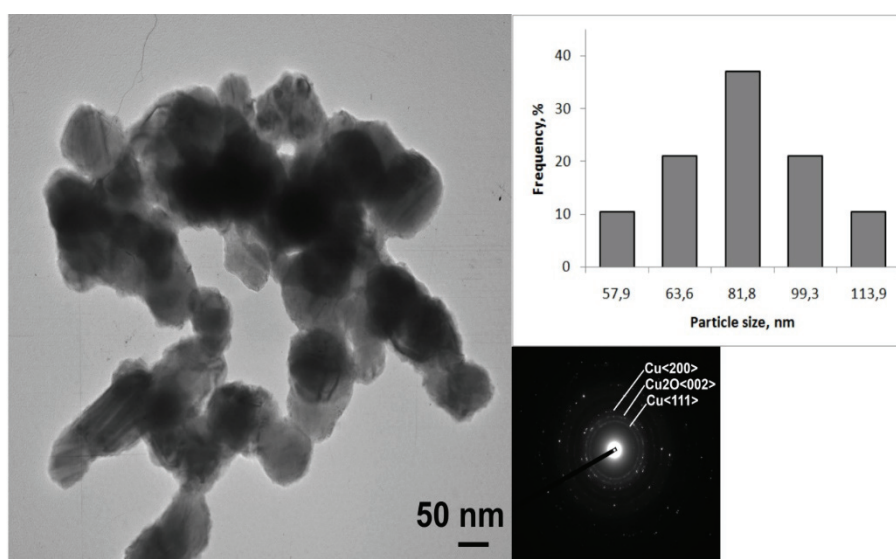


Fig. S-5. TEM image, SAED image and histogram of the size distribution of Cu/Cu<sub>2</sub>O NPs prepared by the MW-assisted polyol method at 185 °C. See text for details.

The lattice parameter  $a$  and interplanar spacing  $d$  for the obtained Cu-based NPs, calculated from the XRD and SAED data, are summarized in Table I. By comparing the structural quality of NPs arising from the different methods of synthesis, it has to be admitted that the cubic CuO NPs did not possess sig-

nificant structural defects. This was not a case for the Cu/Cu<sub>2</sub>O particles, where different types of defects, such dislocations, twins and stacking faults, were found.

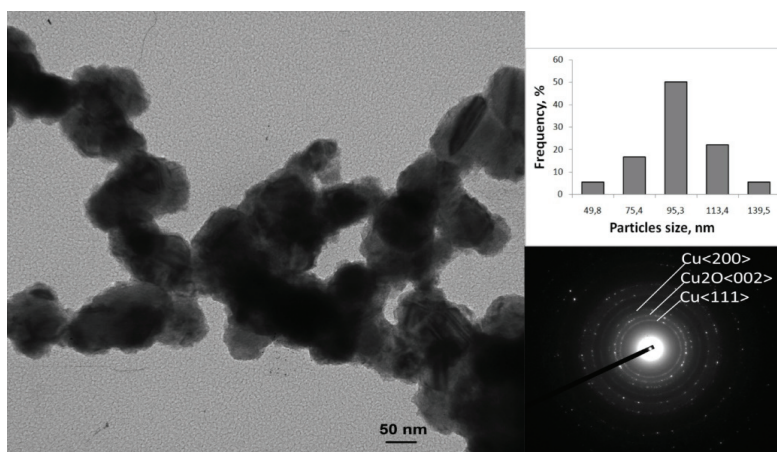


Fig. S-6. TEM image, SAED image and histogram of the size distribution of Cu/Cu<sub>2</sub>O NPs prepared by the MW-assisted polyol method at 200 °C. See text for details.

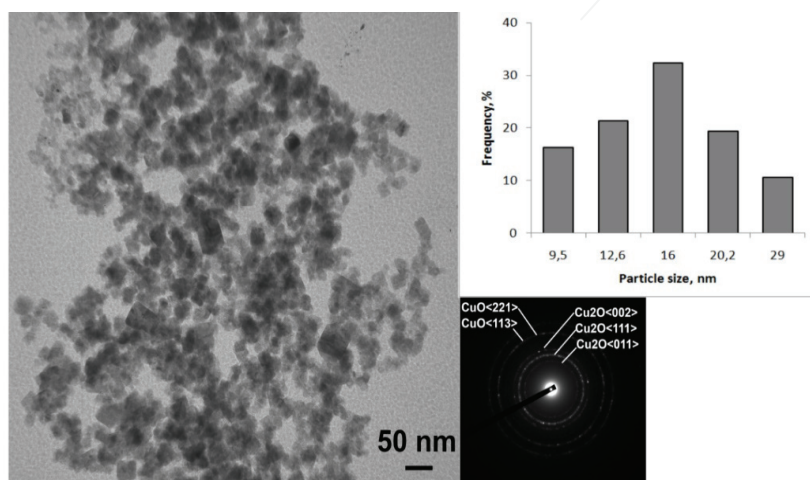


Fig. S-7. TEM image, SAED image and histogram of the size distribution of Cu<sub>2</sub>O/CuO NPs prepared by the borohydride synthesis. See text for details.

The calculated characteristic values (Table I) are in good agreement with each other and comply well with structural data known from the literature for copper-based NPs.

The optical properties of the obtained samples were measured on a Shimadzu UV-2600 UV-Vis spectrophotometer in the diffuse reflectance mode using an integration sphere accessory. Small amounts of the samples were mixed

homogeneously with BaSO<sub>4</sub> powder and filled in a standard optical cuvette. The optical cuvette filled with pure BaSO<sub>4</sub> was used as the reference. Care was taken to ensure a snug fit of the cuvette and the window of integrating sphere to avoid light loss.

The measured optical spectra in % of reflectance values are reported in Fig. S-8a. The difference in the level of reflectance throughout the spectrum originates from the different amounts of the samples available for the measurements. The same spectra were also converted into Kubelka–Munk values and are presented in Fig. S-8b as a function of the wavenumber.

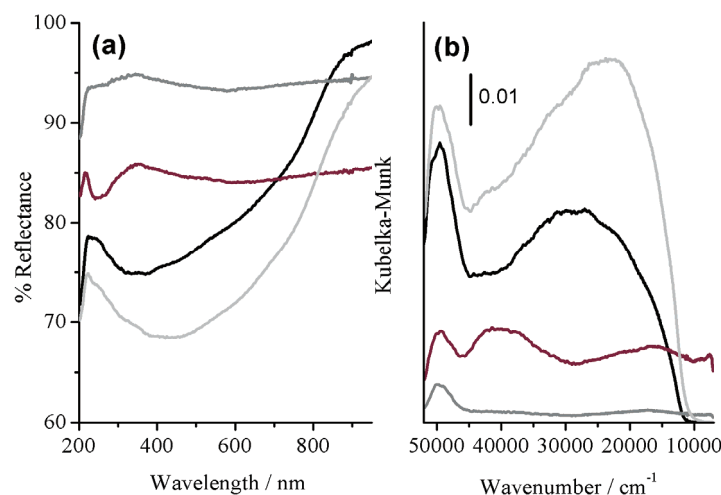


Fig. S-8. a) DRUV–Vis spectra of CuO (black), Cu/Cu<sub>2</sub>O (185 °C, grey), Cu/Cu<sub>2</sub>O (200 °C, dark grey) and Cu<sub>2</sub>O/CuO NPs; b) the same spectra converted into Kubelka–Munk function values and plotted *versus* cm<sup>-1</sup>.

#### REFERENCES

1. K. C. Anyaogu, A. V. Fedorov, D. C. Neckers, *Langmuir* **24** (2008) 4340
2. J. Xiong, Y. Wang, Q. Xue, X. Wu, *Green Chem.* **13** (2011) 900
3. N. Arul Dhas, C. Paul Raj, A. Gedanken, *Chem. Mater.* **10** (1998) 1446
4. D. P. Chattopadhyay, B. H. Patel, *Int. J. Pure Appl. Sci. Technol.* **9** (2012) 1
5. P. Christian, M. Bromfield, *J. Mater. Chem.* **20** (2010) 1135
6. P. Mallick, S. Sahu, *Nanosci. Nanotechnol.* **2** (2012) 71
7. A. A. Radhakrishnan, B. B. Beena, *Indian J. Adv. Chem. Sci.* **2** (2014) 158
8. H. Fan, L. Yang, W. Hua, X. Wu, Z. Wu, S. Xie, B. Zou, *Nanotechnology* **15** (2004) 37
9. Z. Wu, M. Shao, W. Zhang, Y. Ni, *J. Cryst. Growth* **260** (2004) 490
10. Y. Sui, W. Fu, H. Yang, Y. Zeng, Y. Zhang, Q. Zhao, Y. Li, X. Zhou, Y. Leng, M. Li, G. Zou, *Cryst. Growth Des.* **10** (2010) 99
11. B. K. Koo, *Bull. Korean Chem. Soc.* **22** (2001) 113
12. A. B. Lever, *Inorganic Electronic Spectroscopy*, 2<sup>nd</sup> ed., Elsevier, Amsterdam, 1984, p.p. 553–57 and 636–638
13. K. Nakamoto, *J. Phys. Chem.* **64** (1960) 1420
14. K. Sone, P. Krumholz, H. Stammreich, *J. Am. Chem. Soc.* **77** (1955) 777.